Biosensors and Bioelectronics 52 (2014) 403–410

Contents lists available at ScienceDirect

Biosensors and Bioelectronics

journal homepage: www.elsevier.com/locate/bios

Electrochemical immunosensor based on ensemble of nanoelectrodes for immunoglobulin IgY detection: Application to identify hen's egg yolk in tempera paintings

Fabio Bottari [a], Paolo Oliveri [b], Paolo Ugo [a,*]

[a] Department of Molecular Sciences and Nanosystems, University Ca' Foscari of Venice, S. Marta 2137, 30123 Venice, Italy
[b] Department of Pharmacy, University of Genoa, Via Brigata Salerno, 13, 16147 Genoa, Italy

ARTICLE INFO

Article history:
Received 5 July 2013
Received in revised form
21 August 2013
Accepted 6 September 2013
Available online 20 September 2013

Keywords:
Immunosensor
Nanoelectrode
Egg yolk
IgY
Voltammetry
Tempera paint

ABSTRACT

A nanostructured electrochemical biosensor for detecting proteins of interest in work of art, in particular in tempera paintings, is presented. To determine egg yolk we focus here on the determination of immunoglobulin IgY. The transducers are nanoelectrode ensembles (NEEs), prepared via membrane templated electroless deposition of gold. Because of their geometrical and diffusion characteristics, NEEs are characterized by significantly low detection limits, moreover they display the capability of capturing proteins by interaction with the polycarbonate membrane of the NEE. At first, the proteic component of the paint is extracted by ultrasonication in an aqueous buffer, then IgY is captured by incubation on the NEE. The immunoglobulin is detected by treatment with anti-IgY labeled with horse radish peroxidase (Anti-IgY-HRP). The binding of the Anti-IgY-HRP is detected by recording the electrocatalytic signal caused by addition of H_2O_2 and methylene blue. The sensor detection capabilities are tested by analyzing both paint models, prepared in the lab, and real samples, from paintings of the XVIII–XX century. Multivariate exploratory analysis is applied to classify the voltammetric patterns, confirming the capability to differentiate egg-yolk tempera from other kind of tempera binders as well as from acrylic or oil paints.

© 2013 Elsevier B.V. All rights reserved.

1. Introduction

In the field of conservation of cultural heritage, the availability of analytical information on the materials used to produce works of art is crucial. As far as ancient paintings are concerned, the identification of the composition of painting layers furnishes valuable information on the pictorial technique used, authenticity, possible superimposition of later pictorial or varnish layers. All this information is necessary to guide the restoration intervention and to indicate the most suitable conservation conditions.

To this aim, many analytical methods based on the use of advanced instrumentation are presently available. However few tools allow the quick but reliable analysis of small samples performed directly in restoration laboratories by conservation scientists.

A painting is a complex analytical matrix composed by frame, support, priming and preparation, painting and finishing layers. The pictorial layer itself is a complex system composed by pigments (i.e. insoluble metal oxides or salts, organic pigments or lacquers) kept together by a binder. The nature of the binder determines the working behavior of the paint and the final characteristics of the work of art, not only from an esthetic viewpoint, but also as far as durability and conservation are concerned. The binders most commonly used by Western artists include animal glue, casein, egg, drying oils, resins, natural gums and, more recently, synthetic materials such as acrylic polymers and others.

A particularly important painting technique is the tempera technique. This term indeed includes a wide range of painting media based on the use of water dispersible binders which, upon drying, become insoluble. The use of tempera techniques spans from the beginning of Christian era (for miniatures and religious icons) to modern painters (e.g. Böcklin, Giorgio de Chirico, Luigi Tito etc.) up to contemporary artists. The most classical tempera technique was described by Cennino Cennini in his XV century book *"Il Libro dell'Arte"* and it is based simply on mixing the finely grounded pigments with egg yolk. Other tempera techniques use whole egg or egg white, alone or mixed with flour or animal glue. Many artists used also to mix oily components to the classical tempera binders.

From an analytical viewpoint, identifying proteins from different animal sources is not an easy task. One approach is based on sequencing and identifying proteins on the basis of the presence of specific chemical components, using expensive spectroscopic (Casadio and Toniolo, 2001; Doménech-Carbò, 2008; Prati et al., 2010) and chromatographic or hyphenated mass spectrometric techniques (Colombini and Modugno, 2004; Marinach et al., 2004; Doménech-Carbò, 2008). An alternative approach is based on

* Corresponding author. Tel.: +39 041 234 8503; fax: +39 041 234 8594.
E-mail address: ugo@unive.it (P. Ugo).

0956-5663/$ - see front matter © 2013 Elsevier B.V. All rights reserved.
http://dx.doi.org/10.1016/j.bios.2013.09.025

molecular recognition methods which exploit the reactivity of specific molecules present in the binder. Recently, immunosensors have been developed with the purpose of determining the presence of egg as pictorial binder. The use of antibodies in conservation science is not new; dating back to the 1960s–70s (Jones, 1962; Johnson and Packard, 1971). More recently, an immunofluorescence microscopy (IFM) method was proposed to identify ovalbumin (Kockaert et al., 1989) and casein (Ramírez-Barat and de la Viña, 2001); while Heginbotham et al. (2006) used both IFM and ELISA for the identification of ovalbumin. Assays based on chemiluminescence (Dolci et al., 2008; Sciutto et al., 2011) have been developed and many different natural compounds were detected by using ELISA or IFM (Vagnini et al., 2008; Cartechini et al., 2010; Palmieri et al., 2011). These researches opened new prospects for the application of immunosensors to the identification of pictorial binders, however they are targeted to detect ovalbumin, a protein present in high amount in egg albumen and yolk (Mann, 2007; Mann and Mann, 2008). A limit is that those methods cannot discriminate between albumen or whole egg tempera from egg yolk tempera.

In order to develop a sensor able to give specific information on the presence of egg yolk as the binder, in the present study we focus on a different analyte, namely, the glycoprotein immunoglobulin IgY which is the main serum immunoglobulin in chicken (Carlander et al., 1999) and, in chicken eggs, is present in the yolk at concentration of 5–10 mg mL^{-1} (Chalghoumi et al., 2009; Dias da Silva and Tambourgi, 2010). It has a molecular mass of about 180 kDa and its isoelectric point ranges between 5.7 and 7.6 (Chalghoumi et al., 2009). The IgY maintains its stability in a wide range of pH (from 4 to 12) while the thermal denaturation of the protein occurs only above 70 °C. For these reasons, IgY is a suitable candidate to be exploited as a tracer useful to detect the presence of egg yolk in a sample.

The transducers used by us for developing IgY immunosensor, are the nanoelectrode ensembles (NEEs). NEEs are prepared via template electroless deposition of gold within the pores of a polycarbonate (PC) track-etched membrane; the characteristics of the membranes (pore density and pore diameter) determine the voltammetric response of the electrodes (Menon and Martin, 1995; Ugo et al., 1996). When the boundaries of radial diffusion layers of each nanoelectrode overlap, the so called total overlap (TO) diffusion regime is achieved. NEEs prepared from commercial available track etched PC membranes typically operate under the TO regime. Under this regime, a peak dependant faradic current is recorded which is proportional to the geometric area (A_{geom}), while the double layer charging current (the background current) depends only on the active area (A_{act}).

The high ratio between faradic and double layer charging current reflects in very high S/N ratios so that NEEs are characterized by detection limits 2–3 orders of magnitude lower than those of macrolectrodes with the same geometric area (Brunetti et al., 2000; Ugo and Moretto, 2007). For biosensing purposes, another advantage of NEEs is the possibility of binding organic macromolecules, like proteins, to the PC of the electrode ensemble. On the surface of PC membrane there are several carboxylic groups, which interact with the amino terminations of amino-acids (Rucker et al., 2005; Silvestrini et al., 2011). Several biosensors have been recently developed exploiting this characteristic (Zamuner et al., 2008; Pozzi Mucelli et al., 2008; Silvestrini et al., 2013).

The detection scheme used in the present work is based on the protein binding capability of the PC of the NEEs and it is summarized in Scheme 1.

In step (A), IgY is captured by the NEE surface. In step (B), after blocking with BSA, the IgY captured by the NEE surface is incubated with anti-IgY labeled with HRP (Anti-IgY-HRP). Finally, in step (C), the presence of the label HRP, is detected by adding the enzyme substrate (namely, H_2O_2) and methylene blue (MB) as a suitable redox mediator (Pozzi Mucelli et al., 2008). At first the paint models prepared using recipes found in the classical treatise "*Il Libro dell'Arte*" of Cennino Cennini (1370-1440) as well as the recipes used by the modern Venetian painter Luigi Tito (1907-1991) were analyzed. The sensor was finally applied to characterize real samples taken from paintings spanning a time lag from XVIII to XX century.

Multivariate exploratory analysis was applied to the voltammetric profiles. The outcomes confirm that the information embodied in the signals is functional to characterize samples on the basis of the nature of the binder present in the pictorial media.

2. Materials and methods

Electrochemical measurements were carried out at room temperature with a CH660 potentiostat using a three-electrodes cell

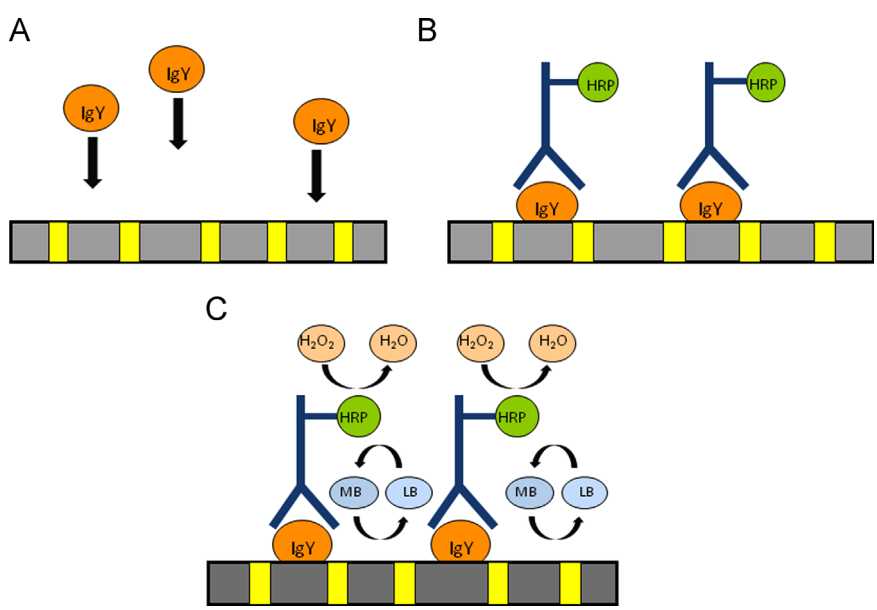

Scheme 1. Schematic representation of the analytical protocol.

equipped with a platinum counter electrode and an Ag\AgCl (KCl-saturated) reference electrode; the NEE was used as the working electrode. The polycarbonate template membranes are supplied by SPI Pore Filter (47 mm diameter, pore thickness 6 μm, pore diameter 30 nm, pore density 6×10^8 pores cm^{-2}). IgY (Chrome Pure IgY, whole molecule) was from Jackson Immunoresearch Laboratories; Anti-IgY-HRP was from Immunology Consultants Laboratory and Bovine Serum Albumin (BSA) was from Sigma-Aldrich. All other chemicals were reagent grade and used without further purification. NEEs were prepared by template gold electroless deposition in PC track-etched membranes according to the procedure developed by Menon and Martin (1995) and following updates (Pereira et al., 2006; De Leo et al., 2007; Ugo and Moretto, 2007). See Supplementary data for details.

2.1. Paint model samples

All paint model samples were prepared mixing the binder with Yellow Ocher ($Fe_2O_3 \cdot H_2O$). A single paint layer was applied on pure cellulose paper, using two tempera recipes found in *"Il Libro dell'Arte"* and three recipes from the painting notes of the Venetian painter Luigi Tito (1907-1991), summarized in Table S1, Supplementary data.

The analysis were performed also on sample of commercial oil (Maimeri) and acrylic (Liquitex) paint layers. The real samples were taken from painting belonging to private collections. List of samples and paintings are reported in Table 1.

2.2. Analytical protocol

The analyses were carried out on paint samples (10 mg for paint models, 1 mg for real paintings) dispersed in 1 mL of 0.1 M phosphate buffer, pH 7, and treated by ultrasonication for 2 h, to extract the proteinaceous compounds. Afterward the following procedure was adopted:

- Ten microliters of the extraction solution were deposited on the surface of a NEE and incubated for 30 min at room temperature, in a humidity chamber made by a sealed Petri's plate with wet filter paper on the bottom. Proteins, like IgY, are expected to bind on the carboxylic groups present on the PC surface (Zamuner et al., 2008; Pozzi Mucelli et al., 2008).
- The NEE was rinsed three times with 1 mL of phosphate buffer.
- The NEE was dipped in a blocking solution (1% bovine serum albumin in phosphate buffer) for 30 min at room temperature on an orbital shaker plate.
- The electrode was rinsed three times with 1 mL of phosphate buffer.
- Ten microliters of 0.05 mg mL^{-1} Anti-IgY HRP in phosphate buffer were deposited onto the surface of the NEE and incubated for 30 min at room temperature in the humidity chamber.
- The NEE was rinsed three times with 1 mL of phosphate buffer.
- The NEE was dipped in the voltammetric cell containing 0.1 mM MB, 0.1 M phosphate buffer, pH 7.
- The CV was recorded at 50 mV s^{-1}, initial potential 0.2 V, vertex potential −0.6 V.
- 8 μL of 1.2 mM H_2O_2 were added to the electrolyte solution.
- The CV was recorded under the above CV conditions.

2.3. Multivariate exploratory analysis

Multivariate analysis was applied to the whole voltammetric profiles recorded after addition of H_2O_2, considered as instrumental fingerprints of samples analyzed. In more detail, principal component analysis (PCA) was performed as exploratory method (Jolliffe, 2002). See Supplementary data for details.

3. Results and discussion

On the basis of previous studies (Pozzi Mucelli et al., 2008), MB was used as redox mediator suitable to shuttle electrons from NEE to the HRP label, bound to Anti-IgY. The dotted line CV in Fig. 1, recorded at a bare NEE, shows a well resolved reduction peak which, according to previous literature reports (Wopschal and Shain, 1967; Ye and Baldwin, 1988), is attributed to the two electron–one proton reduction of MB to the leuco form (LB). This reduction occurs via a rather complex ECE mechanism (Wopschal and Shain, 1967).

The dashed curve in the same figure shows only minor changes in the CV pattern as a consequence of the treatment of the NEE with IgY, plus BSA as blocking agent and Anti-IgY-HRP. Indeed, the cathodic reduction peak current (Ip_c) decreases slightly as well as the associated anodic reoxidation peak (Ip_a), with Ip_a/Ip_c being close to 1 both at a bare NEE and on the modified NEE. When 1.2 mM H_2O_2 is added to the treated NEE, a dramatic change in voltammetric pattern is detected: the reduction current increases, the reoxidation peak disappears and the CV pattern becomes sigmoidally shaped (full line in Fig. 1). These features agree with the occurrence of an electrocatalytic process, which, on the basis of previous research (Pozzi Mucelli et al., 2008), involves the

Table 1
List of real samples analyzed.

Name	Acronym	Description	Period	IgY presence
Adoration of the Magi	IU1	Painting on panel	XVIII–XIX c.	Positive
	IU2			Positive
Landscape	OU1	Oil on cardboard	First half of XX c.	Negative
Still life	OU4	Oil on plywood	1960s	Negative
Nude	CU1	Sketch on paper	1970s	Positive
Adoration of the Magi	I2	Painting on panel	XVII–XVIII c.	Positive
Wooden torch-holder	RT1	Wooden polychrome sculpture	XVI–XVII c.	Positive
Greek Statue	TO1	Paint on canvas panel	XIXc.	Negative
	TO2			Negative
	TO3			Negative
Child Jesus	BG1	Wooden polychrome sculpture	XVI–XVII c.	Negative
Madonna with child	IR1	Painting on panel	About 1700s	Negative
Commercial oil paint	Oil	Produced by Maimeri	————————	Negative
Commercial acrylic paint	Acr	Produced by Liquitex	————————	Negative
Commercial tempera paint	Tcomm	Produced by Maimer	—————————	Negative

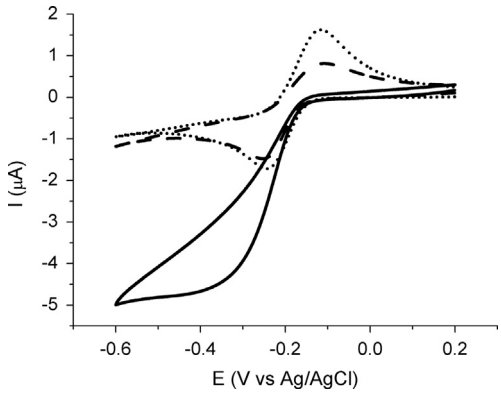

Fig. 1. Cyclic voltammogram in 0.1 mM MB, 10 mM phosphate buffer, pH 7, scan rate: 50 mV s^{-1}. Before incubation (dotted line); after incubation with IgY (1.12 mg mL^{-1}), 1% BSA and Anti-IgY-HRP (0,05 mg mL^{-1}) (dashed line); after addition of 1.2 mM H_2O_2 (full line).

following reactions:

$$MB + 2e^- + H^+ \rightarrow LB \quad (1)$$

$$HRP_{red} + H_2O_2 + 2H^+ \rightarrow HRP_{ox} + 2H_2O \quad (2)$$

$$HRP_{ox} + LB \rightarrow HRP_{red} + MB \quad (3)$$

The CVs recorded at a NEE incubated only with BSA or with BSA and Anti-IgY-HRP (in both cases, with no IgY) overlap with the dashed line in Fig. 1, these CV patterns remain unaltered after addition of H_2O_2. These evidences indicate that, under these conditions, only BSA is eventually adsorbed on the NEE surface (Silvestrini et al., 2011), since the addition of H_2O_2 does not reflect in any further voltammetric change; this excludes any aspecific interaction between Anti-IgY-HRP and the NEE surface. Note that for all the above electrodes, after each incubation, the careful rinsing of the electrodes was performed before running the CV scan.

All these evidences indicate that:

1. IgY is captured by the NEE.
2. IgY, captured by the NEE, reacts efficiently with Anti-IgY-HRP which is consequently bound on the NEE surface.
3. Anti-IgY does not bind on the electrode surface in the absence of IgY.
4. The addition of H_2O_2 causes an electrocatalytic increase of the MB reduction current which could be potentially employed for analytical purposes.

Interestingly, the interactions of the NEE with the sample and with anti-IgY-HRP does not inhibit the cyclic voltammetric detection of MB, so indicating that the proteins are bound mainly on the PC surface, in agreement with previous observations (Pozzi Mucelli et al., 2008), or if they adsorb on the Au surface of the NEE, they do not hinder the MB electrochemical reduction.

A series of experiments were performed incubating different NEEs with solution at different IgY concentrations. After incubation with Anti-IgY-HRP (and carefull rinsing) the electrodes were tested in electrolyte solution (0.1 M phosphate buffer pH 7) containing 0.1 mM MB. CV were recorded at 3 different scan rate (20–50–100 mV/s) before and after the addition of H_2O_2. The parameter analytically useful for identifying IgY is the electrocatalytic current increment (Δi_{cat}) defined as:

$$\Delta i_{cat} = Ip_c(MB)_{\text{with no } H_2O_2} - I \text{ catalytic } (MB)_{\text{with } H_2O_2}$$

At the investigated scan rate (namely 100, 50 and 20 mV s^{-1}), Δi_{cat} shows a sharp dependence on IgY concentration in low concentration range (≤ 0.1 mg mL^{-1}) while it tends to an asymptotic behavior for IgY concentration higher than 0.5 mg mL^{-1}. Such a trend confirm once again the capturing of IgY by the NEE surface since a surface saturation effect is observed. The best compromise between sensibility and peak separation is achieved using a scan rate of 50 mV s^{-1}. (See Fig. S1 in Supplementary data). Concerning the optimization of Anti-IgY-HRP concentration, experiments performed at different concentrations with a constant IgY concentration (0.02 mg mL^{-1}) indicated that the increase of Anti-IgY concentration from 0.02 to 0.05 mg mL^{-1} reflects in an approximately four-fold increase in Δi_{cat}. There is no further increase for higher concentration so suggesting 0.05 mg mL^{-1} Anti-IgY-HRP as the optimum concentration.

3.1. Paint model samples

The main binders examined in model samples were egg yolk, albumen, commercial linseed oil and commercial acrylic. While for the egg yolk and albumen tempera the water extract was clear and it was applied on the electrode without any further treatment, for the oil and acrylic sample, the extract appeared turbid. Preliminary experiments indicated that the direct application of such turbid extract on the NEE compromised the functioning of the electrode. This problem was overcome by centrifugation of the extract to precipitate the particles and obtaining a clear surnatant which was applied on the NEE.

After blocking, the electrodes were incubated with Anti-IgY-HRP, accurately washed and used as working electrode in the electrochemical cell containing phosphate buffer and MB. The voltammetric pattern recorded for the 4 extract and in different steps of the analytical process, are shown in Fig. 2.

The dotted line CVs in Fig. 2 shows the MB signal recorded at NEE before incubation with the extraction solution; these curves are shown as reference CVs. The dashed lines report the CVs recorded at NEE after incubation with the extract samples, blocking with BSA and incubated with Anti-IgY-HRP. Finally, the full line CVs refer to voltammograms recorded after adding 1.2 mM H_2O_2.

Fig. 2A shows that for the yolk tempera (TYolk) extract, an electrocatalytic behavior is clearly observed when H_2O_2 is added. On the other hand, Fig. 2B indicates that, for the albumen tempera (TAlb), the voltammogram maintains the reoxidation peak and the reduction current grows only slightly, so excluding the occurrence of the electrocatalytic sequence which involves Anti-IgY-HRP and H_2O_2 and electrogenerated LB.

These results indicate that the reaction between IgY and Anti-IgY-HRP gives a positive response only for the egg yolk tempera and not for the egg white extract. Indeed, IgY is present in the egg yolk and not in the albumen.

Fig. 2C and D shows that a completely different behavior is observed after incubation and immunoreaction of the oil (acronym: Oil) and acrylic paint sample (Acr). For Oil, the CV recorded at the NEE in the absence of H_2O_2 differs quite significantly for the reference curve obtained at a bare NEE. The cathodic peak current increases as well as ($E_p - E_{p\backslash 2}$) values and $\Delta E_p = Ep_f - Ep_b$ separation, where E_p is the peak potential, $E_{p/2}$ is the half peak potential and the subscripts f and b refer to signals recorded in the forward and backward sweep, respectively. Interestingly, this pattern does not change upon addition of 1.2 mM H_2O_2. These evidences indicate that Anti-IgY-HRP is not bound onto the NEE, since IgY is not present. Moreover, the large peak-to-peak separation, together with the sloping shape of the voltammetric peaks detected in Fig. 2C and D, suggest increased capacitance and resistance of the NEE, which could be due to adsorption or etching of the NEE surface by some component of the extract. In any case,

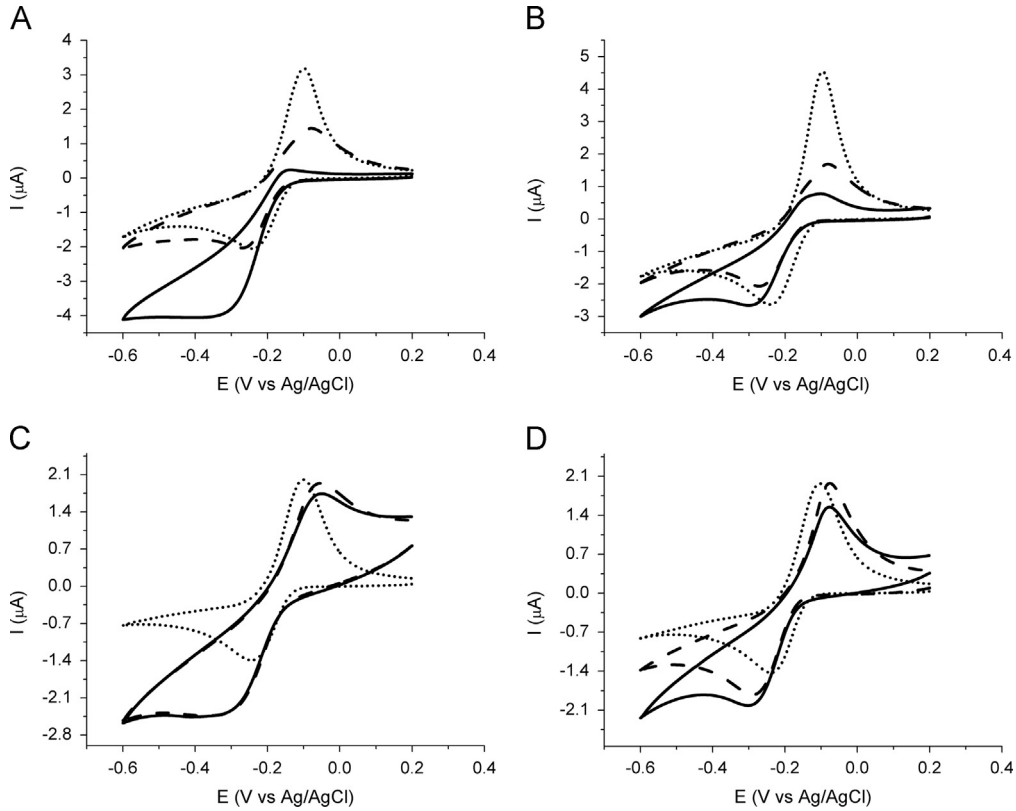

Fig. 2. Cyclic voltammograms recorded before incubation (dotted line); after incubation with extraction solution, 1% BSA and Anti-IgY-HRP conjugated (0,05 mg mL^{-1}) (dashed line); after addition of 1.2 mM H_2O_2 (full line). (A) Yolk tempera, (B) Albumen tempera, (C) Oil, and (D) Acrylic. Other conditions as in Fig. 1.

these features do not change by adding H_2O_2, therefore, they are not related to any IgY/Anti-IgY-HRP interaction.

The Acr sample displays a behavior intermediate between the albumen and the oil sample, with a slight increase in cathodic peak current after incubation and a very light further increase after addition of H_2O_2. Conversely, the anodic peak remains always well detectable. These slight effects due to the H_2O_2 addition to the albumen and acrylic samples are probably related to some minor side reaction between H_2O_2 and other components of the extract, whose effect is anyway very different and much less important than the one caused by the electrocatalytic cycle described by reactions 1–3. It is worth pointing out that also model samples of *tempera grassa* (TGr and T1, see Table S1), egg and flour tempera (T2), flour and glue tempera (T3) were examined by the same procedure. Relevant CVs are reported in Supplementary data. For these cases of complex binders it is observed that the *tempera grassa* and egg and flour tempera show an electrocatalytic behavior comparable to that of yolk tempera, while flour and glue tempera do not. This agrees with the evidence that *tempera grassa* and egg and flour tempera contain egg yolk while flour and glue tempera does not. A sample of modern tempera paint commercially available (Tcomm) gives negative response, suggesting that the binder does not contain egg yolk.

3.2. Application to real artworks

The analyses on real paint samples were carried out on several paintings that belong to private collectors. Four samples of wooden icons of XVII–XVIII century and 2 samples of wooden polychrome sculptures from XVI–XVII century were analyzed. Three samples from the same painting from XIX century were also analyzed. These samples were taken from different layers: one from the ground layer, one from the original painting layer and the last one from a recent repainting. To complete the set of real samples, also three samples from modern paintings were analyzed; namely, two oil on cardboard and one sketch on paper, both of XX century. The list of samples are reported in Table 1, together with relevant sample acronyms; the CVs and a brief description of all samples are reported in the Supplementary data. Fig. 3 shows typical voltammograms representative of the CV behavior recorded on some real paint sample; two from paintings (IU1 and OU4) and two for wooden polychrome sculptures (BG1 and RT1).

The samples IU1 and RT1 (Fig. 3A and B) show an electrocatalytic current increase, when H_2O_2 is added to the NEEs incubated with the sample extract and anti-Ig-Y-HRP, as above described. The detection of the electrocatalytic current agrees with the presence of egg yolk in these paint samples; note that also another sample (IU1) from the same artwork gave a similar result (see CVs in Supplementary data). On the other hand, the CVs relevant to different samples, namely RT1 and BG1 (Fig. 3C and D, respectively), show CV patterns different from those of samples IU1 and OU4, but comparable with those of the oil paint model samples. The ΔE_p and $(E_p–E_{p/2})$ values increase sensibly together with the cathodic peak current; note that the addition of H_2O_2 does not cause any further change, so suggesting that IgY/Anti-IgY-HRP were not captured by the NEE.

The analyses carried out on paint model samples and samples from real paintings provided sets of analytical data, suitable for a more precise definition of the type of binder that is being analyzed. The main discriminating factor which indicates whether a sample contains an egg yolk based binder or not is the appearance of electrocatalytic process between MB and HRP. However, also other characteristics gained for the CV patterns can be helpful to further characterization of the sample. Table 2 lists four of these characteristics useful to this aim, all inserted in a tentative diagnostic scheme.

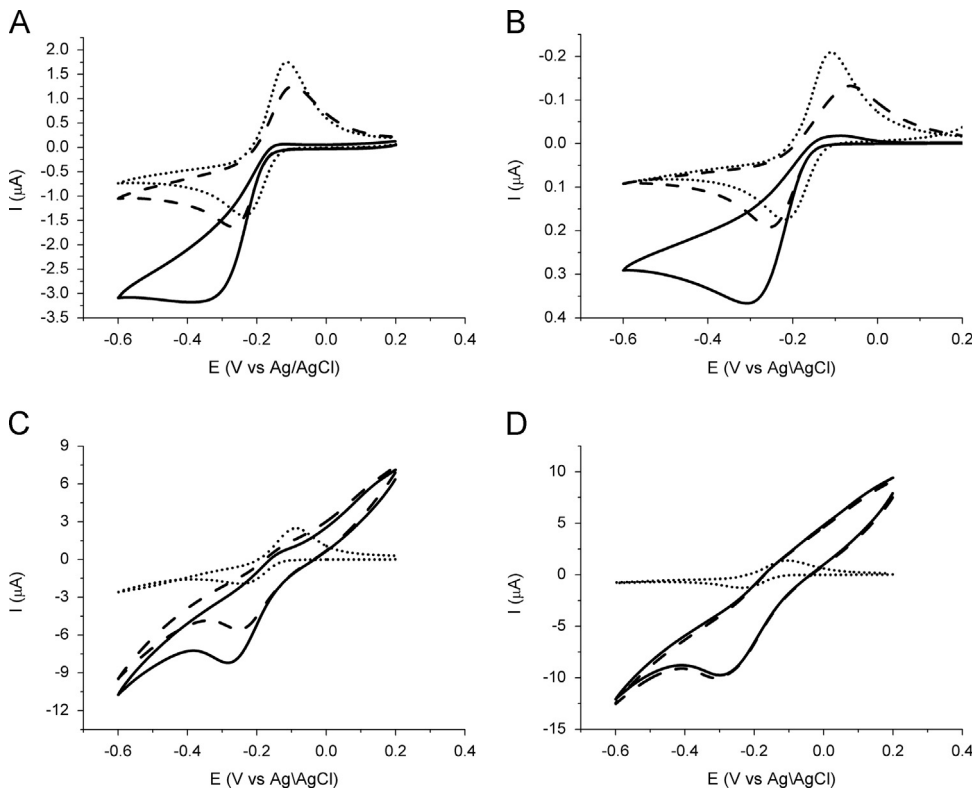

Fig. 3. Cyclic voltammograms recorded before incubation (dotted line); after incubation with extraction solution, 1% BSA and Anti-IgY-HRP conjugated (0,05 mg mL^{-1}) (dashed line); after addition of 1.2 mM H_2O_2 (full line). (A) IU1, (B) RT1, (C) BG1, and (D) OU4. Other conditions as in Fig. 1.

Table 2
Tentative diagnostic scheme based on the changes in the voltammetric patterns caused by the addition of H_2O_2.

Painting Binder	Cathodic peak	Anodic peak	CV pattern	H_2O_2 effect
Egg-yolk tempera	Significant increase	Disappears	Sigmoidal (catalytic)	Dramatic
Other tempera	Slight increase	Slight decrease	Peak shaped	Almost negligible
Oil	Increase	Almost unchanged	Peak with ohmic distortion	Completely negligible
Acrylic	Slight increase	Slight decrease	Peak shaped	Almost negligible

From the exam of the scheme one can conclude that the convergence of all four factors, allow one to identify the presence of egg yolk in the paint layers. Among the examined samples such a positive convergence was found for samples IU1, IU2, CU1, I2, RT1, T1, T2, TGr and TYolk. Interestingly, this analysis point out that also other binders can be identified by the response the proposed analytical procedure, as it is the case of the oil binder; the CV recorded with the NEE in these samples show indeed the special features represented typically by the dashed and full line in Fig. 3C and D. This is not due to any specific interaction of the NEE with any protein nor antibody, but it is related to a more generic kind of interaction between the NEE and the extract. On the basis of these observations and in order to extract the maximum analytical information for the sample, all the voltammetric data were further examined by performing Principal Component Analysis (PCA), as described below.

3.3. Principal component analysis (PCA)

PCA was applied to the raw voltammetric patterns analyzed as components of a data matrix structured with 24 rows (samples) and 1600 variables (currents measured at each sweep potential). The samples acronym and characteristic are listed in Tables 1 and S1 and in the above text. Both paint model and real artwork samples were included therein, in order to provide a comprehensive overview of the potentiality of the method in characterizing samples on the basis of presence/absence of egg yolk. The voltammograms processed by multivariate analysis were those recorded after addition of H_2O_2.

At first, signals were transformed by means of a standard normal variate (SNV) transform aimed at minimizing unwanted systematic differences among different measurements (Oliveri et al., 2010). Then, data were mean-centred column-wise and submitted to PCA. The score plot on the two lowest-order principal components is shown in Fig. 4A; samples which resulted positive to the egg yolk presence on the basis of the criteria in Table 2, are indicated as squared data points in the plot, while all the other are shown as circled data. A clear differentiation between samples positive to egg yolk vs. negative ones is clearly evidenced by the plot, with both of the principal components being involved in such a differentiation.

By a joint examination of the score plot (Fig. 4A) and the loading plot (Fig. 4B), it is possible to highlight the original variables (namely, the regions of the CVs) that are most involved in the characterization of samples containing egg yolk. They correspond to the current values gained in the −0.3 to −0.5 V potential region, which are found – in the loading plot – to be opposite (with respect to the axis origin) to the direction in which

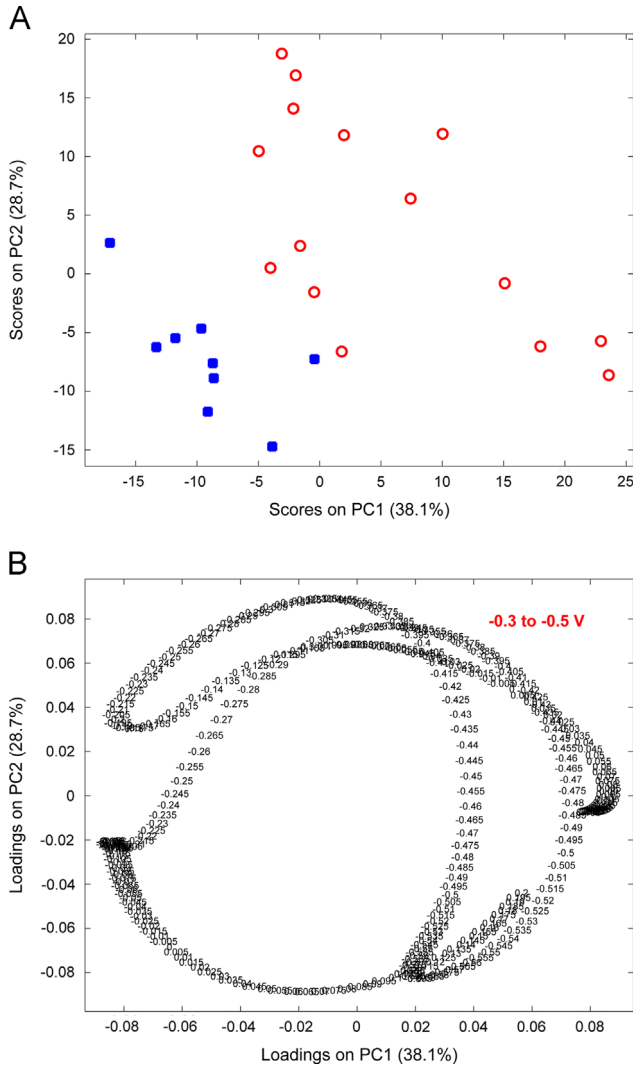

Fig. 4. Graphical output of PCA performed on CV recorded after addition of H_2O_2. (A) Score plot showing the differentiation between positive (solid squares) and negative (circles) samples. (B) Loading plot showing the original variables most involved in the differentiation.

the positive samples are localized within the score plot (solid squares in Fig. 4A).

Such an inverse correspondence is due to the fact that current values are negative in this potential range, which is, indeed, the part of the CV where the rise of the catalytic current is eventually observed.

The outcomes of PCA clearly confirm that the method proposed is a valuable tool for identifying egg yolk tempera in real paint samples of different nature.

4. Conclusions

This approach to the analysis of ancient paint binders is able to conjugate the specificity of immunochemical techniques with the rapid and cost affordable electrochemical detection. The use of a direct approach, in which the antigen is bound directly on the transducer surface, reduces the analytical steps and the reagents required. Another important advantage is the use of NEEs, which furnish well resolved CV patterns, with high S/N ratios and which demonstrate very interesting IgY capturing capability, related to the high affinity of proteins for PC (Silvestrini et al., 2013). From a general bioanalytical and biosensing viewpoint, this is the first report describing an electrochemical immunosensor suitable for IgY detection. This seems an interesting achievement, taking into account the increasing use of IgY for advanced immune diagnostic and immunotherapy (Dias da Silva and Tambourgi, 2010).

Concerning the particular application studied here, i.e. paint binder identification, the analysis of the CVs allows a satisfactory distinction between the patterns obtained from samples containing IgY from those which do not contain such a protein. A reliable data analysis can be performed either using the simple diagnostic scheme illustrated in Table 2 or using a more sophisticated, but more precise PCA method. In principle, if suitable antibodies be available, a similar procedure could be extended also to the detection of other proteins of interest in the field of cultural heritage study and conservation.

Acknowledgments

Financial support by MIUR-Rome, (Project PRIN 2010AXENJ8) is acknowledged. We thank Giovanna Niero (conservator in Noale, Venezia) for providing some of the real samples and for skillful technical support and expertise.

Appendix A. Supplementary material

Supplementary data associated with this article can be found in the online version at http://dx.doi.org/10.1016/j.bios.2013.09.025.

References

Brunetti, B., Ugo, P., Moretto, L.M., Martin, C.R., 2000. Journal of Electroanalytical Chemistry 491, 166–174.
Carlander, D., Stalberg, J., Larsson, A., 1999. Journal of Medical Sciences 104, 179–190.
Cartechini, L., Vagnini, M., Palmieri, M., Pitzurra, L., Mello, T., Mazurek, J., Chiari, G., 2010. Accounts of Chemical Research 43, 867–876.
Casadio, F., Toniolo, L., 2001. Journal of Cultural Heritage 2, 71–78.
Chalghoumi, R., Beckers, Y., Portetelle, D., Théwis, A., 2009. Biotechnology, Agronomy, Society and Environment 13 (2), 295–308.
Colombini, M.P., Modugno, F., 2004. Journal of Separation Science 27, 147–160.
De Leo, M., Pereira, F.C., Moretto, L.M., Scopece, P., Polizzi, S., Ugo, P., 2007. Chemistry of Materials 19, 5955–5964.
Dias da Silva, W., Tambourgi, D.V., 2010. Veterinary Immunology and Immunopathology 135 (2010), 173–180.
Dolci, L.S., Sciutto, G., Guardigli, M., Rizzoli, M., Prati, S., Mazzeo, R., Roda, A., 2008. Analytical and Bioanalytical Chemistry 392, 29–35.
Doménech-Carbò, M.T., 2008. Analytica Chimica Acta 621, 109–139.
Heginbotham, A., Millay, V., Quick, M., 2006. Journal of the American Institute for Conservation 45, 89–105.
Johnson, M., Packard, E., 1971. Studies in Conservation 16, 145–164.
Jolliffe, I.T., 2002. Principal Component Analysis, second ed. Springer, New York.
Jones, P.L., 1962. Studies in Conservation 7, 10–16.
Kockaert, L., Gausset, P., Dubi-Rucquoy, M., 1989. Studies in Conservation 34 (4), 183–188.
Mann, K., Mann, M., 2008. Proteomics 8, 178–191.
Mann, K., 2007. Proteomics 7, 3558–3568.
Marinach, C., Papillon, M.C., Pepe, C., 2004. Journal of Cultural Heritage 5, 231–240.
Menon, V.P., Martin, C.R., 1995. Analytical Chemistry 67, 1920–1928.
Oliveri, P., Casolino, C., Forina, M., 2010. In: Taylor, S. (Ed.), Chemometric Brains for Artificial Tongues. Advances in Food and Nutrition Research, Academic Press, Burlington, pp. 57–117.
Palmieri, M., Vagnini, M., Pitzurra, L., Rocchi, P., Brunetti, B.G., Sgamellotti, A., Cartechini, L., 2011. Analytical and Bioanalytical Chemistry 399, 3011–3023.
Pereira, F.C., Moretto, L.M., De Leo, M., Boldrin Zanoni, M.V., Ugo, P., 2006. Analytica Chimica Acta 577 (1), 16–24.
Pozzi Mucelli, S., Zamuner, M., Tormen, M., Stanta, G., Ugo, P., 2008. Biosensors and Bioelectronics 23, 1900–1903.
Prati, S., Joseph, E., Sciutto, G., Mazzeo, R., 2010. Accounts of Chemical Research 43, 792–801.
Ramírez-Barat, B., de la Viña, S., 2001. Studies in Conservation 46, 282–288.
Rucker, V.C., Havenstrite, K.L., Simmons, B.A., Sickafoose, S.M., Herr, A.E., Shediac, R., 2005. Langmuir 21, 7621–7625.
Sciutto, G., Dolci, L.S., Buragina, A., Prati, S., Guardigli, M., Mazzeo, R., Roda, A., 2011. Analytical and Bioanalytical Chemistry 399, 2889–2897.

Silvestrini, M., Schiavuta, P., Scopece, P., Pecchielan, G., Moretto, L.M., Ugo, P., 2011. Electrochimica Acta 56, 7718–7724.
Silvestrini, M., Fruk, L., Ugo, P., 2013. Biosensors and Bioelectronics 40, 265–270.
Ugo, P., Moretto, L.M., 2007. Template deposition of metal. In: Zoski, C.G. (Ed.), Handbook of Electrochemistry. Elsevier, Amsterdam, pp. 678–709.
Ugo, P., Moretto, L.M., Bellomi, S., Menon, V.P., Martin, C.R., 1996. Analytical Chemistry 68, 4160–4165.
Vagnini, M., Pitzurra, L., Cartechini, L., Miliani, C., Brunetti, B.G., Sgamellotti, A., 2008. Analytical and Bioanalytical Chemistry 392, 57–64.
Wopschal, R.H., Shain, I., 1967. Analytical Chemistry 39, 1527–1534.
Ye, J., Baldwin, R.P., 1988. Analytical Chemistry 60 (20), 2263–2268.
Zamuner, M., Pozzi Mucelli, S., Tormen, M., Stanta, G., Ugo, P., 2008. European Journal of Nanomedicine 1, 33–36.

Supplementary Data

Electrochemical Immunosensor Based on Ensemble of Nanoelectrodes for Immunoglobulin IgY Detection: Application to Identify Hen's Egg Yolk in Tempera Paintings.

Fabio Bottari[a], Paolo Oliveri[b], Paolo Ugo[a]*

[a] Department of Molecular Sciences and Nanosystems, University Ca' Foscari of Venice, Santa Marta 2137, 30123 Venice, Italy

[b] Department of Pharmacy, University of Genoa, Via Brigata Salerno, 13, I-16147 Genoa, Italy

*Corresponding author. Tel.: +39 041 234 8503; E-mail address: ugo@unive.it.

Template electroless deposition and assembly of NEEs

Briefly, after wetting for 2 h in methanol, the track-etched polycarbonate membrane was sensitized into 0.026 M $SnCl_2$, 0.07 M trifluoroacetic acid in 50% methanol in water, for 45 min. Then it was rinsed in methanol, and dipped in 0.029 M $Ag[(NH_3)_2]NO_3$ for 10 min. The membrane was rinsed in methanol and then in water and successively it was immersed into the Au plating bath containing 7.9×10^{-3}M $Na_3Au(SO_3)_2$ in 0.127 M Na_2SO_3, at 0°C. After 20 min, 0.625 M formaldehyde was added to the bath. Electroless deposition was allowed to proceed for 40 min, after which additional 0.625 M formaldehyde was added. After a total of 24 h of plating, the golden membrane was rinsed with water and immersed for 6 h in 10% HNO_3, then rinsed again with water and dried. NEEs were assembled as previously described (Ugo and Moretto, 2007). Briefly, a small piece of golden membrane was attached to a suitable conductive substrate; the gold layer on the outer face of the membrane was removed by peeling with scotch tape (so that only the head of the gold nanowires inside the pores will be exposed to solution); all the surface of the NEE, apart a hole of 3 mm diameter (which defines A_{geom} = 0.07 cm^2), was insulated with a film of heat shrinkable plastic film (Monokote by Topflite). Good sealing between the nanoelectrodes and the polycarbonate was assured by finally heating the NEE at 150°C for 15 min (De Leo et al., 2007).

Table S1

Recipes of *tempera* used for paint models

Name	Sample	Source	Composition (in volume)
Yolk tempera	TYolk	Cennino Cennini *"Il Libro dell'arte"*	1 part of Egg yolk 1 part of Water
Egg white tempera	TAlb	Cennino Cennini *"Il Libro dell'arte"*	1 part of Egg white 1 part of Water
Tempera Grassa	TGr	Luigi Tito	1 part of Egg yolk 2 part of Linseed oil
Tempera Grassa	T1	Luigi Tito	1 Egg yolk, 6 part of Water 3 part of Linseed oil ½ part of Arabic Gum ½ part of Rosin
Egg and flour tempera	T2	Luigi Tito	1 Whole Egg 2 part of Linseed oil 8 part of Water 1 part of Flour ¼ part of Honey ½ part of Vinegar
Flour and glue tempera	T3	Luigi Tito	3 part of Flour 1 part of Linseed oil 14 part of Water ½ part of Vinegar ¼ part of Honey 1 part of Rabbit-skin glue

Fig.S1 Dependence of electrocatalytic current increment on IgY concentration (0,1 0,05 0,02 mg mL $^{-1}$)) for different scan rate (20 – 50 – 100 mV s^{-1}).

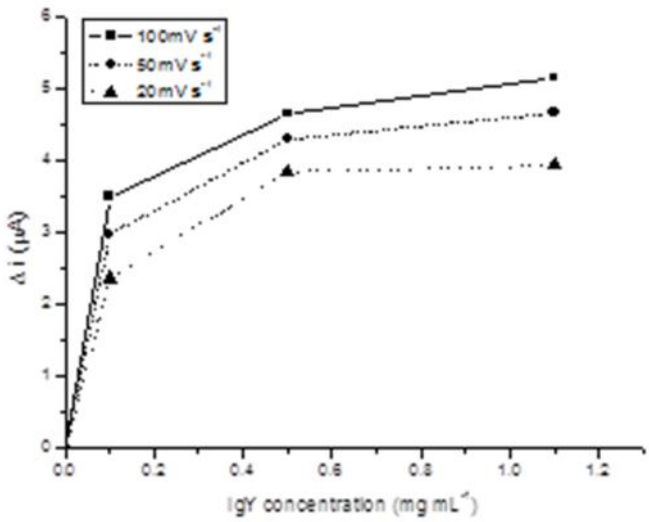

Multivariate exploratory analysis

Principal component analysis (PCA) is based on the assumption that a high variability (i.e., a high variance value) is synonymous with a high amount of information. For this reason, it searches for the maximum variance direction, in the multidimensional space of the original data, passing through the data centroid. The maximum variance direction represents the first principal component. The second principal component is the direction which keeps the maximum variance among all directions orthogonal to the first component. The process continues with the identification of the subsequent components: it may stop at reaching a variance cut-off value or continue until all the variability enclosed in the original data has been explained (Jolliffe, 2002).
Each sample can be projected in the space defined by the new variables: the coordinate values obtained are called scores.
The principal components are expressible as linear combinations of the original variables: the coefficients which multiply each variable are called loadings. They represent the cosine values (director cosines) of the angles between the principal components and the original variables. These values may vary between -1 and +1, indicating the importance in defining a given principal component: the larger their absolute value, the larger the contribution of the corresponding original variables to the component.
One of the key features of PCA is its high capability for representing large amounts of complex information by way of simple bidimensional or tridimensional plots. In fact, the space described by two or three principal components can be used to represent the objects (score plot) and the original variables (loading plot). Since principal components are orthogonal variables, no duplicate information is shown in the plots.

Voltammograms on different kinds of tempera samples

Figure S2 reports the CV patterns recorded on samples of: (A) "tempera grassa (oil-tempera)" (B) egg and flour tempera (C) fluor and glue tempera, recorded operating with the same experimental conditions as those described in the main text for egg yolk tempera samples (see Fig. 2 and related text).

Fig.S2. Cyclic voltammograms in 0.1 mM MB, 10 mM phosphate buffer, pH7, scan rate: 50 mV s^{-1}; before incubation (dotted line); after incubation with extraction solution, 1% BSA and Anti-IgY-HRP (0.02 mg mL^{-1}) (dashed line); after addition of 1.2 mM H_2O_2 (full line). (A) Tempera grassa (B) Egg and flour tempera (C) Fluor and glue tempera.

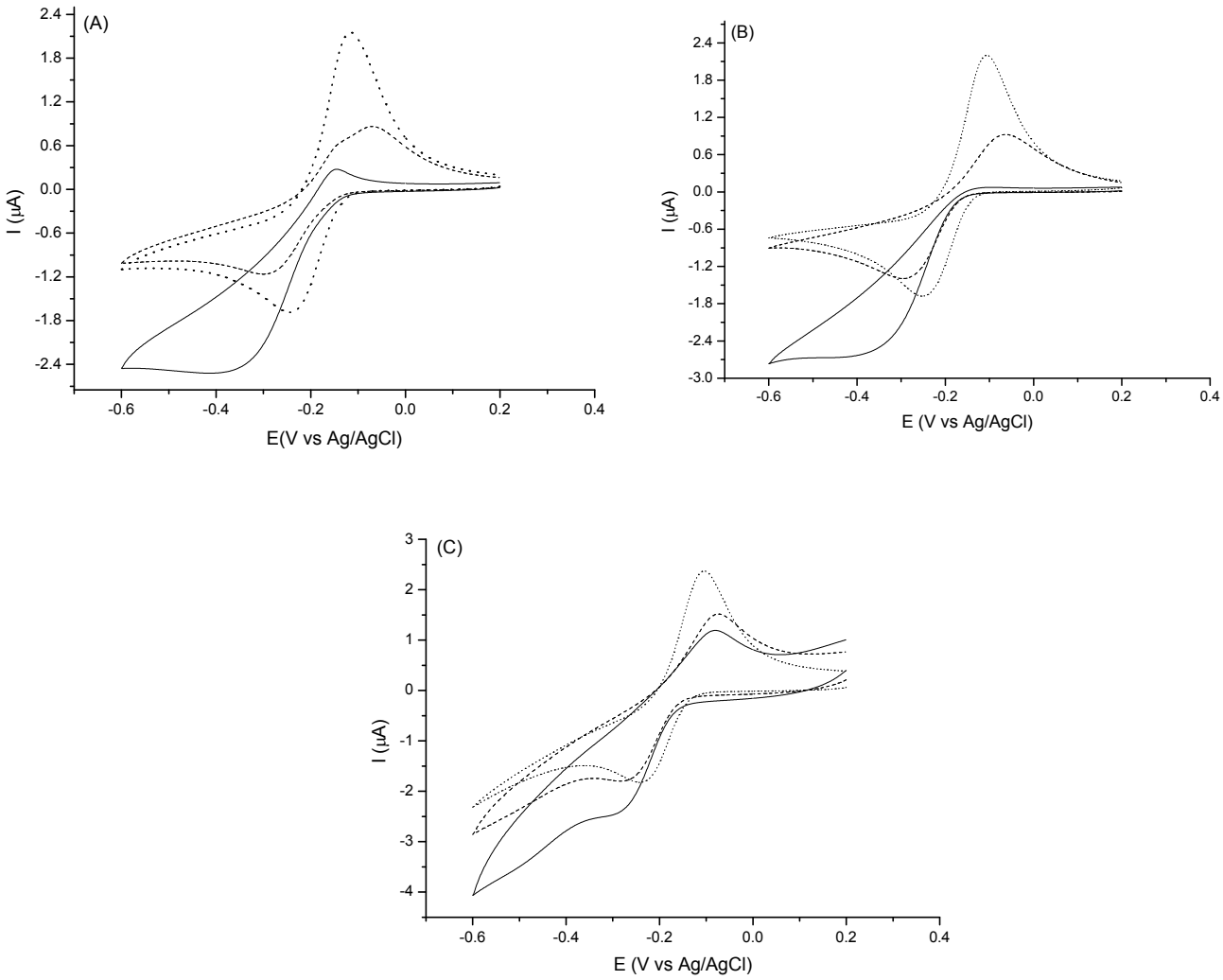

Voltammograms on real paintings

In the following, the CVs recorded on real samples are reported, together with a photograph and the work of art from which the samples were taken. Relevant experimental conditions are described in section 3.2 of the main text.

Fig. S3. Cyclic voltammograms in 0.1 mM MB, 10 mM phosphate buffer, pH7, scan rate: 50 mV s^{-1}; before incubation (dotted line); after incubation with extraction solution, 1% BSA and Anti-IgY-HRP (0.02 mg mL^{-1}) (dashed line); after addition of 1.2 mM H_2O_2 (full line). Sample IU2 from *Adoration of the Magi.*

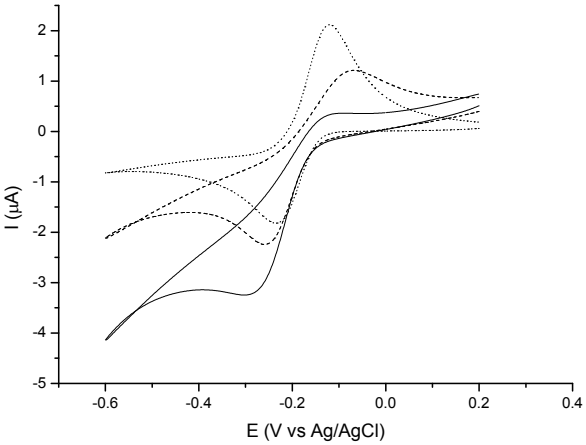

Fig.S4 Cyclic voltammograms in 0.1 mM MB, 10 mM phosphate buffer, pH7, scan rate: 50 mV s^{-1}; before incubation (dotted line); after incubation with extraction solution, 1% BSA and Anti-IgY-HRP (0.02 mg mL^{-1}) (dashed line); after addition of 1.2 mM H_2O_2 (full line). Sample OU1 from *Landscape.*

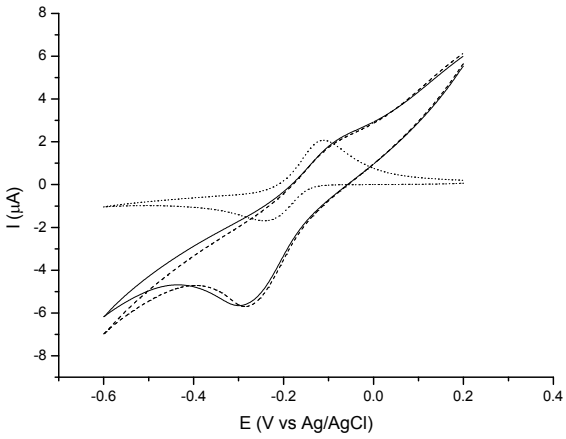

Fig.S5. Cyclic voltammograms in 0.1 mM MB, 10 mM phosphate buffer, pH7, scan rate: 50 mV s^{-1}; before incubation (dotted line); after incubation with extraction solution, 1% BSA and Anti-IgY-HRP (0.02 mg mL^{-1}) (dashed line); after addition of 1.2 mM H_2O_2 (full line). Sample CU1 from *Nude.*

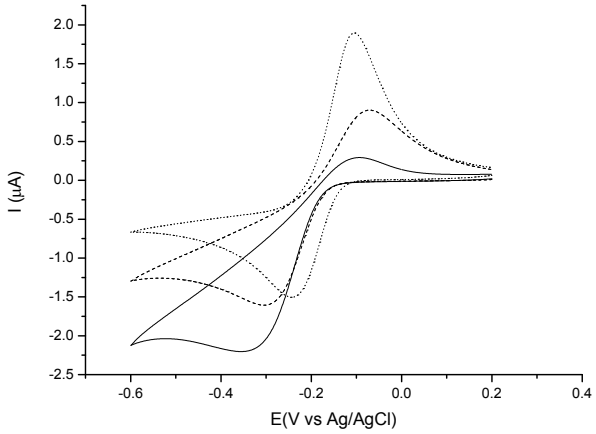

Fig.S6. Cyclic voltammograms in 0.1 mM MB, 10 mM phosphate buffer, pH7, scan rate: 50 mV s^{-1}; before incubation (dotted line); after incubation with extraction solution, 1% BSA and Anti-IgY-HRP (0.02 mg mL^{-1}) (dashed line); after addition of 1.2 mM H_2O_2 (full line). Sample I2 from *Adoration of the Magi.*

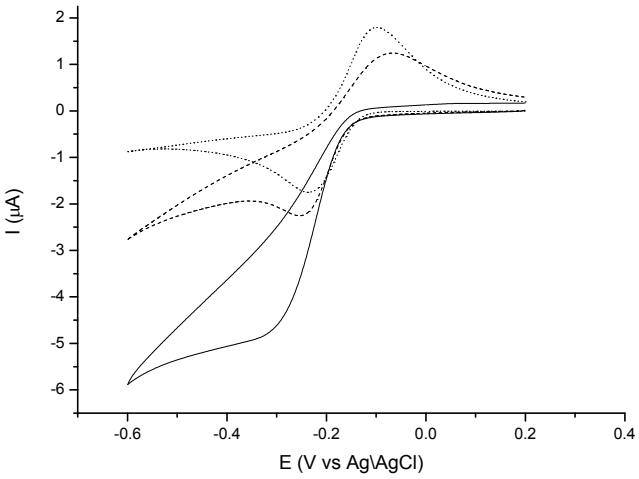

Fig.S7. Cyclic voltammograms in 0.1 mM MB, 10 mM phosphate buffer, pH7, scan rate: 50 mV s^{-1}; before incubation (dotted line); after incubation with extraction solution, 1% BSA and Anti-IgY-HRP (0.02 mg mL^{-1}) (dashed line); after addition of 1.2 mM H_2O_2 (full line). Sample IR1 from *Madonna with Child.*

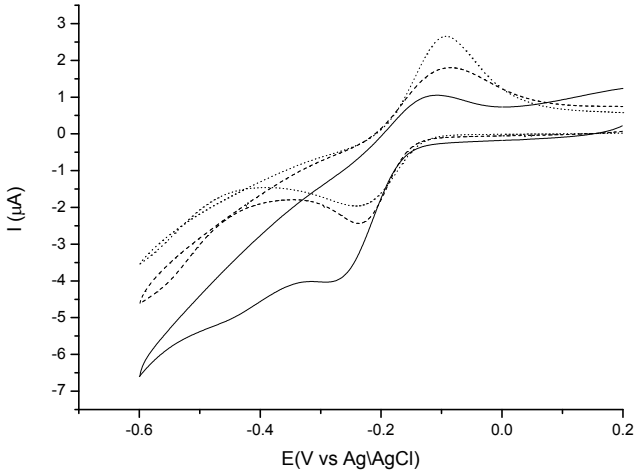
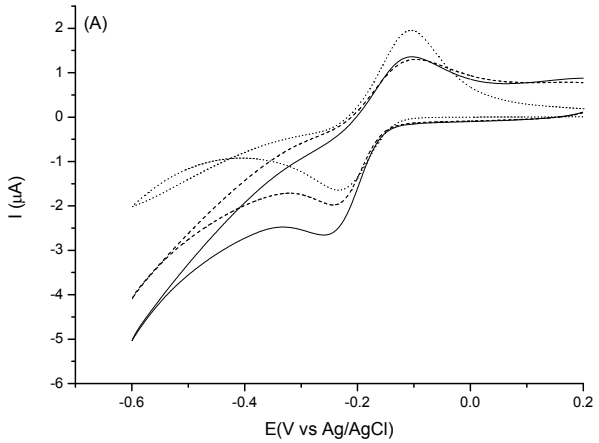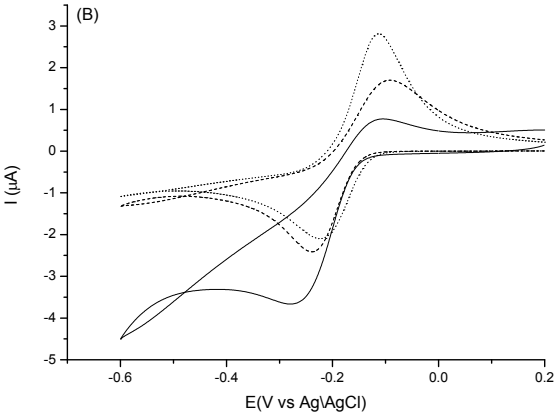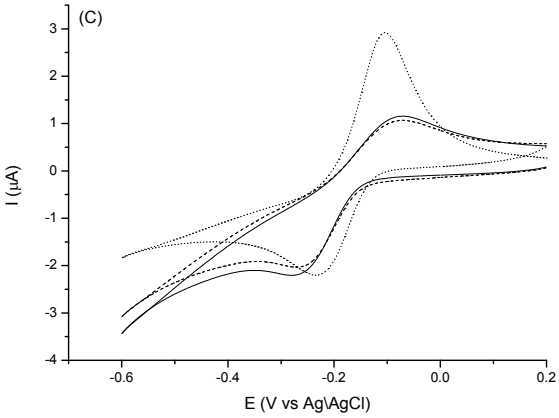
Fig.S8. Cyclic voltammograms in 0.1 mM MB, 10 mM phosphate buffer, pH7, scan rate: 50 mV s^{-1}; before incubation (dotted line); after incubation with extraction solution, 1% BSA and Anti-IgY-HRP (0.02 mg mL^{-1}) (dashed line); after addition of 1.2 mM H_2O_2 (full line). Sample TO1 (A) TO2 (B) TO3 (C) from *Greek Statue.*